Interphase chromosomes in *Arabidopsis* are organized as well defined chromocenters from which euchromatin loops emanate

Paul Fransz*†, J. Hans de Jong‡, Martin Lysak*, Monica Ruffini Castiglione§, and Ingo Schubert*

*Institute of Plant Genetics and Crop Plant Research (IPK), D-06466 Gatersleben, Germany; ‡Laboratory of Genetics, Wageningen University, Arboretumlaan 4, 6703 BD, Wageningen, The Netherlands; and §Department of Plant Sciences, Istituto di Mutagenesi e Differenziamento, Consiglio Nazionale delle Ricerche, 56100 Pisa, Italy

Edited by Mark T. Groudine, Fred Hutchinson Cancer Research Center, Seattle, WA, and approved August 26, 2002 (received for review May 31, 2002)

Heterochromatin in the model plant *Arabidopsis thaliana* is confined to small pericentromeric regions of all five chromosomes and to the nucleolus organizing regions. This clear differentiation makes it possible to study spatial arrangement and functional properties of individual chromatin domains in interphase nuclei. Here, we present the organization of *Arabidopsis* chromosomes in young parenchyma cells. Heterochromatin segments are organized as condensed chromocenters (CCs), which contain heavily methylated, mostly repetitive DNA sequences. In contrast, euchromatin contains less methylated DNA and emanates from CCs as loops spanning 0.2–2 Mbp. These loops are rich in acetylated histones, whereas CCs contain less acetylated histones. We identified individual CCs and loops by fluorescence *in situ* hybridization by using rDNA clones and 131 bacterial artificial chromosome DNA clones from chromosome 4. CC and loops together form a chromosome territory. Homologous CCs and territories were associated frequently. Moreover, a considerable number of nuclei displayed perfect alignment of homologous subregions, suggesting physical transinteractions between the homologs. The arrangement of interphase chromosomes in *Arabidopsis* provides a well defined system to investigate chromatin organization and its role in epigenetic processes.

The eukaryotic nucleus features a complex differentiation of heterochromatic and euchromatic domains, each having specific nuclear functions (1, 2). Although genetically identical, somatic cells may differ in the nuclear organization because of changes in the amount and distribution of heterochromatin. The most common type is constitutive heterochromatin, which is permanently condensed, transcriptionally inert, rich in repetitive DNA, and capable of silencing genes of adjacent euchromatin (3, 4). In many species, it occurs around centromeres and nucleolus organizing regions (NORs). A second type of heterochromatin involves chromosome regions that, in specific cells, become compact and transcriptionally inactive on remodeling of chromatin. The molecular mechanism of chromatin remodeling currently is being unraveled in several eukaryotes. Covalent modifications of the histone tails appear to play an important role (5). For example, deacetylation followed by methylation at lysine 9 of histone H3 recruits heterochromatin protein (HP1) and leads to chromatin condensation and gene inactivation. These events have been reported for yeast (6, 7), mammals (6, 8), *Drosophila* (9), and plants (10), indicating the widespread occurrence of this process.

A positional relationship between heterochromatinization and gene silencing was shown earlier in flies (11, 12) and mammals (13, 14). Silencing of certain genes seems to be correlated with sequestration of the gene to a heterochromatic compartment involving specific proteins (13), whereas activated enhancers suppress silencing of genes by preventing their localization at heterochromatin (14). To understand how chromosomes function within interphase nuclei, it is essential to investigate individual chromatin domains in a well defined system. Microscopic studies of human nuclei have revealed chromosome-specific domains or territories, in which transcription appears to take place predominantly at or near the surface of compact chromatin domains (15). However, because of the complex nature of human chromosomes, it remains difficult to establish a clear relationship between DNA sequence, the higher-order structure of chromosomes, and gene regulation. *Arabidopsis thaliana* ($n = 5$) may provide an appropriate system to study large-scale organization of chromatin domains. Its chromosomes display small, conspicuous heterochromatin segments that mark the position of each centromere and of the NORs of chromosomes 2 and 4 (Fig. 1*A*; see ref. 16). They contain most of the repetitive DNA sequences, comprising ≈15% of the entire genome (17). The centromere core consists predominantly of a 180-bp tandem repeat and several transposon-like sequences (18, 19). The flanking heterochromatin regions are enriched in dispersed, repetitive transposon sequences and differ structurally and functionally from the centromere core (20).

In interphase nuclei, heterochromatin is organized as clearly distinguishable chromocenters (CCs). These are visible as dark spots with phase-contrast microscopy or as bright, fluorescent domains after 4′,6-diamidino-2-phenylindole staining. Already in 1907, Laibach (21) discovered that the number of CCs in *Arabidopsis* corresponds to that of chromosomes. How the linear organization of *Arabidopsis* chromosomes corresponds with the arrangement of heterochromatin and euchromatin compartments within interphase nuclei was still unknown. Here, we identified and characterized individual heterochromatin domains by using fluorescence *in situ* hybridization (FISH) and immunolabeling. We demonstrate the existence of euchromatin loop structures around these domains and visualize homologous association of chromosome regions.

Materials and Methods

Plant Material. Young rosette leaves and immature flower buds were harvested from *A. thaliana* accessions Wassileskija, C24, Zurich, and Landsberg and fixed in ethanol/acetic acid (3:1).

Probe Labeling. The following DNA clones were used: 25S rDNA (22), 5S rDNA (23), pAL1 (18), CIC yeast artificial chromosome clones (24), IGF and TAMU bacterial artificial chromosomes (BACs) (25, 26), and pAtT4 (27). BACs from the long-arm 4L were pooled into eight groups as described in ref. 28. All DNA clones were labeled individually with either biotin-dUTP or

This paper was submitted directly (Track II) to the PNAS office.

Abbreviations: NOR, nucleolus organizing region; FISH, fluorescence *in situ* hybridization; BAC, bacterial artificial chromosome; CC, chromocenter.

†To whom correspondence should be sent at the present address: Swammerdam Institute for Life Sciences, University of Amsterdam, Kruislaan 318, 1098 SM, Amsterdam, The Netherlands. E-mail: fransz@science.uva.nl.

www.pnas.org/cgi/doi/10.1073/pnas.212325299

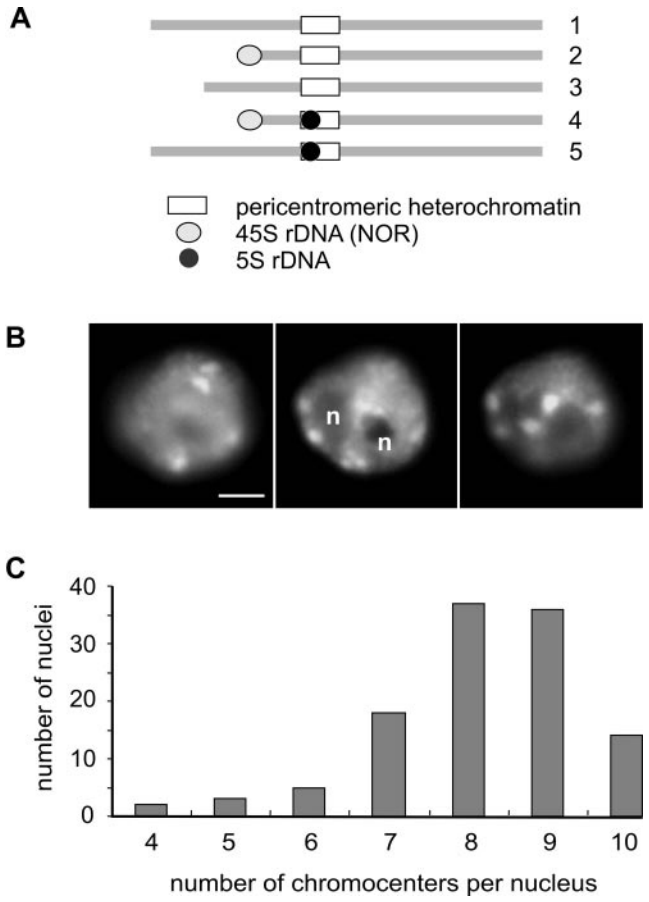

Fig. 1. Heterochromatin distribution in *A. thaliana*. (*A*) Ideogram showing the five chromosomes with 5S and 45S loci. (*B*) Three optical sections of a paraformaldehyde-fixed interphase nucleus stained with 4′,6-diamidino-2-phenylindole showing CCs near the periphery and the nucleolus. (Bar = 2 μm.) (*C*) Distribution of the number of CCs per nucleus.

digoxigenin-dUTP by using a nick translation kit (Boehringer Mannheim).

FISH Analysis. FISH experiments were carried out as described (16, 28). FISH preparations were examined on a Zeiss Axioplan by using 4′,6-diamidino-2-phenylindole, FITC, and Texas red fluorescence filter blocks. Images were recorded with a conventional camera or charge-coupled device camera (Photometrics) by using IP-LABS software and digitally processed with Adobe PHOTOSHOP software. The positions of hybridization signals and CCs were analyzed in relation to each other. Partly or completely overlapping fluorescent foci were interpreted as colocalizing or associating, whereas other situations were considered as separate positions of the regions.

Immunolabeling of Methylated DNA. Slide preparations were baked at 60°C for 30 min, denatured in 70% formamide, 2× SSC, and 50 mM sodium phosphate, pH 7.0, washed in ice-cold PBS 2 × 5 min, incubated in 1% BSA in PBS (10 mM sodium phosphate, pH 7.0/143 mM NaCl) for 30 min at 37°C, and subsequently incubated with mouse antiserum (1:50) raised against 5-methylcytosine (29) in the same buffer for 30 min at 37°C. Mouse antibodies were detected as described for FISH detection.

Immunolabeling of Histone Isoforms H4Ac5 and H4Ac8. Nuclei were isolated from 500 mg of leaves by chopping the tissue with a razor blade in 1 ml of ice-cold 10 mM Tris·HCl, pH 9.5/10 mM

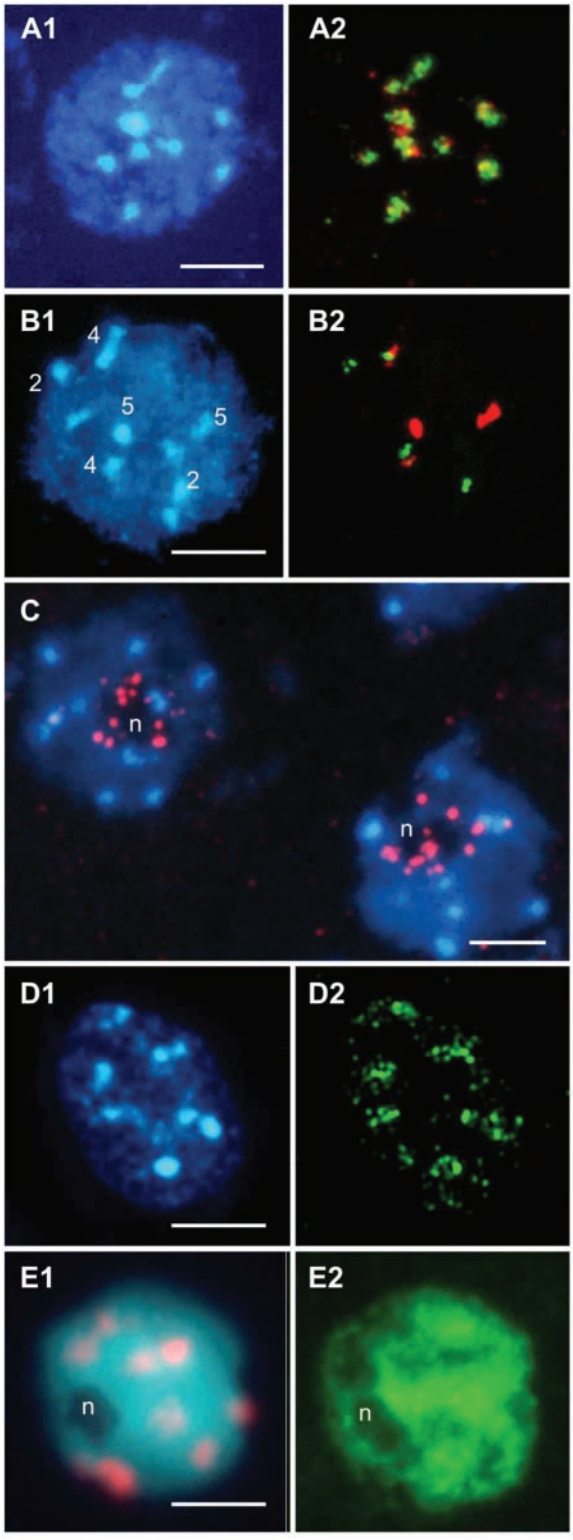

Fig. 2. Identification and characterization of CCs by FISH and immunolabeling to nuclei of the accession Wassileskija. All preparations were counterstained with 4′,6-diamidino-2-phenylindole (blue). (*A*) FISH with centromeric pAL1 (red) and pericentromeric F17A20 repeats (green). (*B*) FISH with 5S (red) and 45S rDNA (green). Numbers correspond to chromosomes. (*C*) FISH with the telomeric sequence (red) yielded clustered signals around the nucleolus (n). (*D*) Immunolabeling with antibodies against 5-methylcytosine (green). (*E*) Immunolabeling with antibodies against histone H4Ac5 (green) and FISH with the centromeric pAL1 (red). [Bar = 2 μm (*E*) and 5 μm (*A–D*).]

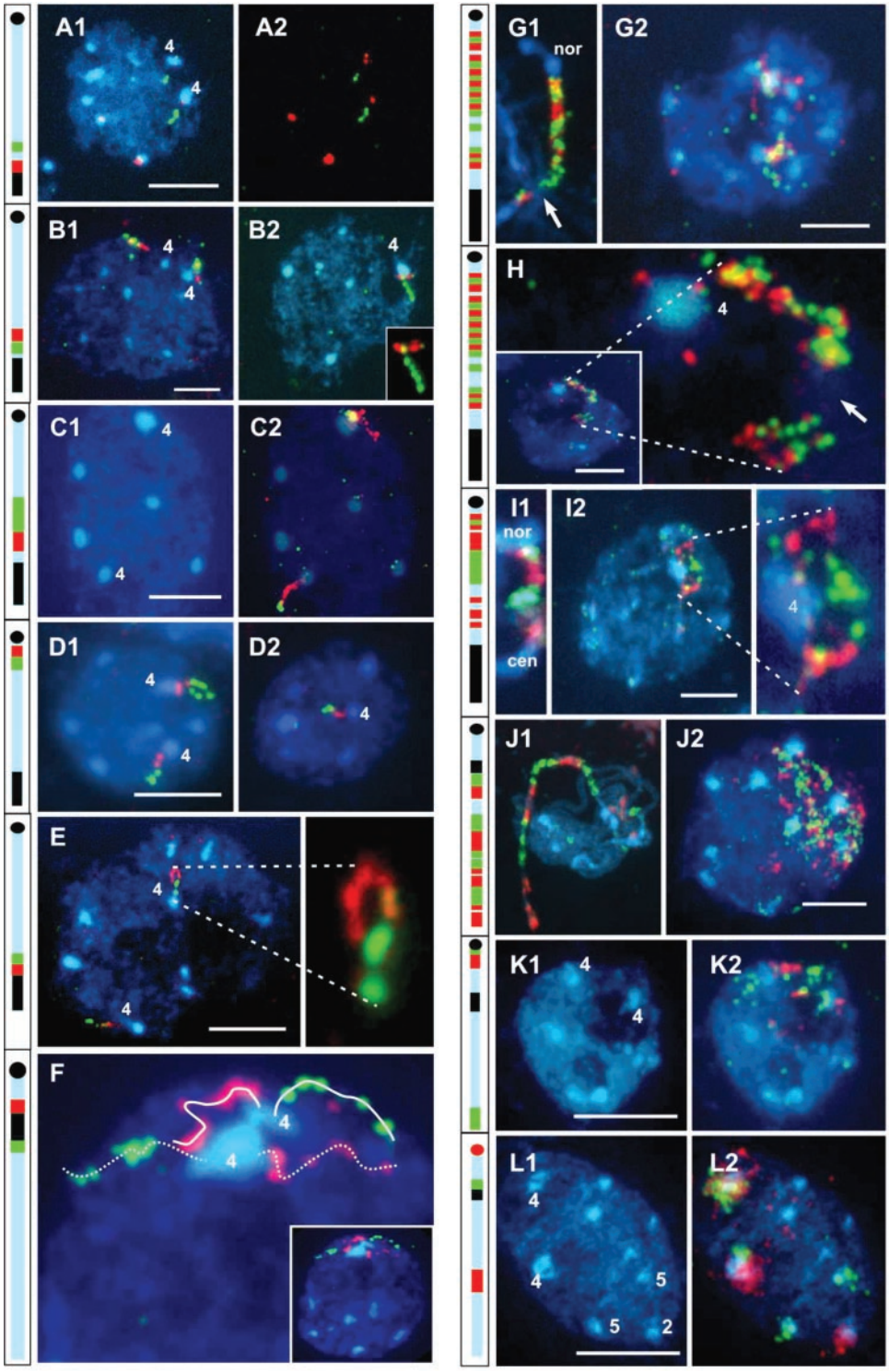

Fig. 3. FISH localization of chromosome 4 regions in nuclei of the accessions Landsberg (*A* and *B*), Wassileskija (*C* and *J*), Zurich (*D*), and C24 (*E*– *I*, *K*, and *L*). Diagrams on the left indicate the map position of the DNA clones in chromosome 4. Solid circle and rectangle represent NOR4 and pericentromere 4, respectively. (*A*) BAC clone T4B21 (green) is outside CC4, whereas 5S rDNA (red) colocalizes with CC4 and CC5. (*B*) Two contiguous BAC clones T4B21 (green) and T1J1 (red). Note the position of the distal T1J1 relative to T4B21 and CC4. B2 shows a FISH signal of aligned, homologous regions. Note the inverse order of centromere-T1J1-T4B21 signals. (*C*) Two contiguous yeast artificial chromosome clones, 8B1 (green) and 7C3 (red), localize close to CC4. 8B1 (980 kb) covers the heterochromatic knob hk4S, whereas the adjacent 7C3 (480 kb) is located in the proximal euchromatin. The difference in chromatin density between the two regions is illustrated by the length of the signals. (*D*) Two contiguous BACs, F5J10 (green) and F6N15 (red), from the distal end of chromosome arm 4S, showing separate (*Left*) and associated (*Right*) homologous regions. Note the loop structure in one of the homologs. (*E*) Two adjacent BACs, T19B17 (green) and the proximal T27D20 (red), form a small loop structure (see magnification). Note the difference in array position between the signals of the two homologs. (*F*) Pools of five BACs from the short (red) and long (green) arm adjacent to the pericentromere. The interrupted and uninterrupted white lines represent the hybridization patterns of the homologous regions. (*G* and *H*) Pachytene chromosome and interphase nuclei hybridized with a mix of 18 BACs covering 2 Mbp of chromosome arm 4S. During interphase, chromosome arm 4S forms either a cloud of small loops (*G2*) or a single giant loop (*H*). The arrows indicate corresponding nonlabeled

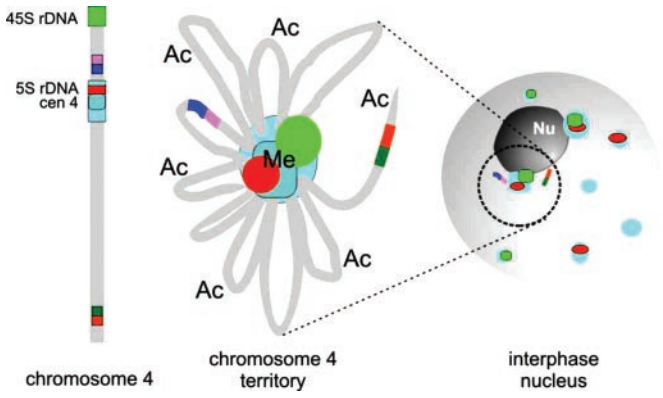

Fig. 4. CC–loop model for the organization of chromosome 4 in *Arabidopsis* nuclei. Heterochromatic regions compartmentalize into one CC, whereas euchromatin forms 0.2- to 2-Mbp loops around this CC. CCs contain heavily methylated DNA (Me), whereas euchromatin loops are enriched in acetylated histone H4 (Ac). The colored blocks represent interstitial, contiguous BACs that show different positions relative to the CC depending on the loop organization.

EDTA/100 mM KCl/0.5 M sucrose/4 mM spermidine/1.0 mM spermine/0.1% (vol/vol) 2-mercaptoethanol (NIB). The homogenate was filtered through 20-μm mesh nylon and fixed by adding an equal amount of 4% paraformaldehyde in PBS. After 30 min, the suspension was centrifuged in an Eppendorf centrifuge at 2,500 rpm for 4 min at 4°C, and the pellet was resuspended in 50 μl of NIB. Three microliters of suspension was pipetted to a clean slide, dried at 4°C, and postfixed in 4% paraformaldehyde in PBS for 30 min at room temperature. Slides were incubated in 1% BSA in PBS at 37°C for 30 min followed by incubation with rabbit antisera R41 and R232 (30) raised against histone H4, which was acetylated at lysines 5 and 8, respectively, in the same buffer (31). Rabbit antibodies were detected with antiserum conjugated with fluorescein as described for FISH detection.

Results

CCs Contain Major Tandem Repeats. Interphase nuclei from immature parenchyma cells contain up to 10 conspicuous CCs, located near the nuclear periphery and the nucleolus (Fig. 1 *B* and *C*). FISH with the probes pAL1 and F17A20, containing centromeric and pericentromeric repeats (16, 32), yielded signals exclusively at all CCs (Fig. 2*A*), indicating that CCs represent the nuclear domains of (peri-)centromeric heterochromatin. FISH with 45S rDNA, which maps to NOR2 and NOR4, and with 5S rDNA, which maps to CEN4 and CEN5 (see Fig. 1*A*), revealed nearly all 5S (99%, $n = 427$) and 45S (97%, $n = 353$) signals at CCs. The occurrence of two green (45S), two red-green (5S + 45S), and two red signals (5S) in many nuclei (Fig. 2*B*) suggests compartmentalization of the terminal 45S rDNA segments of chromosome arms 2S and 4S together with the centromeres of the corresponding chromosomes. The compartmentalization of NOR4 and CEN4 also was confirmed by FISH with unique DNA clones that flank NOR4 (see below and Fig. 3*D*). Unlike (peri-)centromeric and ribosomal repeats, most telomeric sequences hybridized outside CCs, in the vicinity of nucleoli (Fig. 2*C*). Only two to four telomere signals colocalized with CCs and most likely represent the ends of chromosome arms 2S and 4S, which contain the NORs. Hence, *Arabidopsis* chromosomes do not expose a "Rabl" orientation, with telomeres and centromeres at opposite nuclear poles as observed in many plant species (33, 34).

CCs Contain Hypermethylated DNA and Weakly Acetylated Histone H4. Methylated DNA generally is associated with transcriptionally silent domains and often found in heterochromatic regions. Immunolabeling with antibodies against 5-methyl-cytosine showed that CCs contain most of the heavily methylated DNA (Fig. 2*D*) and, therefore, likely represent transcriptionally silent domains of *Arabidopsis* nuclei. Because acetylation of histones H3 and H4 often corresponds with transcriptional activity, we applied antibodies against histones H4Ac5 and H4Ac8 (30). Both labeled specifically euchromatin, whereas CCs were unlabeled (Fig. 2*E*), supporting the view that CCs are transcriptionally inactive.

Euchromatic Loops Emanate from the CC. Compartmentalization of the distal NORs 2 and 4 with the corresponding centromeres raised the question of whether the interstitial euchromatin domains also are closely associated with the centromere. We therefore hybridized BACs from the short arm of chromosome 4 and established their position relative to CC4. With BAC T4B21, which maps to the proximal euchromatin (20), the majority of the signals (84%, $n = 58$) were outside the CCs (Fig. 3*A*), whereas only 16% colocalized with CC4. BACs from other euchromatin regions, including those flanking the NOR and the pericentromere, yielded comparable results (Fig. 3 *B–F*), although the frequency of colocalization with CC4 varied between the regions (unpublished data). We concluded that the short arm of chromosome 4 forms at least one euchromatic loop. To investigate whether more than one loop indeed may emanate from the CC, we studied the nuclear positions of the BACs T4B21 and T1J1, the latter mapped distally from T4B21 in the accession Landsberg (19). If the short arm consists of a single loop, we expect a positional array of CC-T4B21-T1J1. This was observed for 38% ($n = 50$) of the signals (Fig. 3*B*). However, 30% showed the reversed order, indicating the presence of more than one euchromatic loop between NOR4 and CEN4. In the remaining 32%, the order of signals could not be determined, because of equal distances of both signals to CC4. Similar results were obtained with other DNA probes (Fig. 3*C*). Occasionally, DNA loops spanning up to 185 kb, with a condensation degree of approximately 55 kb/μm, could be observed (Fig. 3 *D* and *E*). Thus, we conclude that the short arm 4S is organized in one or more loops around CC4.

CC and Euchromatic Loops Form a Chromosome Territory. To determine the nuclear position of the entire chromosome arm 4S in relation to CC4, we simultaneously hybridized 18 BACs covering 2 Mbp. In most cases (83%, $n = 64$), this hybridization yielded a dispersed pattern of signals around CC4, suggesting an arrangement of euchromatin into several small loops (Fig. 3*G*). However, in the remaining 17%, we observed a single loop spanning the major part of this arm (Fig. 3*H*). The looped arrangement was easily deduced from the pattern of red-green signals, which corresponded with the FISH pattern on pachytene

regions in the nucleus and the pachytene chromosome. (*I*) Pachytene chromosome and interphase nucleus hybridized with a mix of 17 BACs that differs from *G* in labeling pattern. Note that the homologous arms, 4S, in *H* and *I* are perfectly aligned. (*J*) Pachytene chromosome and interphase nucleus hybridized with a mix of 113 BACs from the long-arm 4L. (*K*) Twelve long-arm BACs are labeled in green and map to the distal end. In interphase nuclei, this region may associate with CC4, which supports the conclusion that loop formation also occurs in the long arm. The short arm is visualized by 13 BACs in red and 1 distal BAC in green. (*L*) The middle region of the long arm (10 red BACs) may also associate with CC4, which is identified by 5S (green) and 45S rDNA (red) probes. CC2 and CC5 are identified by 45S and 5S rDNA, respectively. In this case, one CC2 colocalizes with its homolog or with CC4. (Bar = 5 μm.)

Table 1. Percentage of nuclei (n = 115) with associated or separate homologous CCs based on 5S rDNA and 45S rDNA hybridization signals

CC	Associated CCs* (one signal)	Separate CCs (two signals)
CC2 (green)	74.8	25.2
CC4 (red-green)	18.3†	81.7‡
CC5 (red)	10.4	89.6

*Association of homologous CCs or CCs with homologous rDNA repeats.
†In this case, homologous CC4s are closely associated.
‡The percentage of nuclei with three red-green (5S + 45S) signals is low (2%) and indicates that association of CCs2 and -5 is rare.

chromosomes. Similar loops were detected with another BAC mix from the same arm (Fig. 3*I*). This supports the conclusion that chromosome arm 4S is arranged as one or multiple euchromatin loops.

We also investigated the position of the long arm 4L by using 113 individually labeled BACs and observed dispersed signals, representing either separated (79%, n = 52 nuclei) or associated (21%) territories of 4L homologs (Fig. 3*J*), which is in accordance with the association frequency of homologous CC4s (see below). The dispersed pattern of hybridization signals suggests multiple loop structures. We could not trace megabase-sized loops spanning the entire long arm. However, when we probed the distal 12 BACs of 4L, we found 29% (n = 68) of the signals closely associated with CC4 that was identified by short-arm BACs (Fig. 3*K*). BACs from the middle of the long arm gave similar results (Fig. 3*L*). This implies that compartmentalization of euchromatic segments with CCs may occur along the entire chromosome 4, forming loop structures around its CC (Fig. 4). FISH experiments with DNA sequences from other chromosomes also showed hybridization signals at and outside the CCs, suggesting a similar CC–loop organization. Within the loops, the degree of chromatin condensation may vary. For example, yeast artificial chromosome 8B1, which covers the heterochromatic knob *hk4S* of the accession Wassileskija (20), is highly condensed (1 Mbp/μm), compared with the adjacent yeast artificial chromosome 7C3 (180 kb/μm) (Fig. 3*C*).

Association of Homologous Territories, CCs, and Euchromatic Regions. The high number (88%) of nuclei with less than 10 CCs (Fig. 1*C*) indicates close association of CCs. To investigate whether homologous or heterologous CCs were involved, we scored the association frequencies of CCs2, -4, and -5 from the 5S rDNA (red) and 45S rDNA (green) hybridization patterns. In 18.3% of the nuclei, we observed a single CC with a red-green signal, indicating association of homologous CC4s (Table 1). A similar association frequency for CC4s (23.2%, n = 56) was found after FISH with the BACs F5J10 and F6N15 that flank NOR4. CC5s showed less and CC2s more frequent association (Table 1). Nonhomologous association between CC2 and CC5 is considered rare, because the percentage of nuclei with three red-green (5S + 45S) signals was low (2%). These results suggest a nonrandom association of homologous CCs or CCs that contain homologous rDNA repeats. Fig. 5 presents the frequency of separate homologous CCs in relation to the number of CCs per nucleus. All homologs are separated in nuclei with 10 CCs, each representing the heterochromatic segments of an individual chromosome. In nuclei with less than 10 CCs, we observed colocalization of CC2 preferentially and of CC1 and/or 3. The latter lack a 5S or 45S signal and, therefore, could not be distinguished from each other. Homologous CC4s and CC5s appear associated especially in nuclei with less than seven separate CCs. These data indicate that homologous CCs associate nonrandomly.

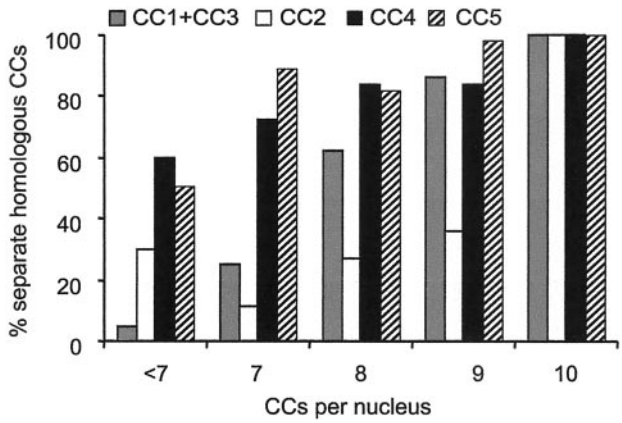

Fig. 5. Histogram showing the percentage of separate homologous CCs. CC1 and CC3, which could not be distinguished from each other, are combined as one group.

We next examined homologous association of individual euchromatic regions by assessing the occurrence of aligned homologous regions from the short arm of chromosome 4. By FISH with at least two contiguous BACs, it is possible to establish the orientation of the target regions. Correct alignments were scored as homologous association. We observed 5–6% (n = 114) perfectly aligned homologous regions spanning 200 kb to 2 Mbp (Fig. 3 *B*, *D*, *H*, and *I*). In all cases, the homologous CC4s colocalized, suggesting that homologous association of euchromatin regions is accompanied by association of heterochromatin.

Discussion

Our study revealed a relatively simple organization of chromosomes within *Arabidopsis* nuclei with chromosome territories consisting of a single repeat-rich, heterochromatic CC, from which gene-rich, euchromatic loops emanate, spanning 0.2–2 Mbp. CCs and loops differ as to the level of DNA methylation and histone H4 acetylation, reflecting the transcriptional inactivity of CCs. This also is supported by strong methylation of lysine 9 of histone H3 only at CCs and of lysine 4 of H3 outside CCs (Z. Jasencakova and W. Soppe, personal communication). The simple arrangement of chromatin and the ability to identify individual CCs and loops makes the *Arabidopsis* nucleus an attractive model with which to study eukaryotic chromosome organization in relation to genomic functions.

Several models of higher-order chromatin structures have been proposed based on microscopic investigation of human interphase chromosomes (2, 15, 35–38). Chromosomes occupy a discrete territory, within which compact chromatin domains are distinguishable from less condensed ones (2, 39, 40). Gene-rich regions are preferentially at the periphery of a chromosome territory, but transcription appears to take place especially at or near the surface of the compact domains (15). It is assumed that 30-nm chromatin fibers emanate as loops from a flexible backbone. How these loops correspond with euchromatin and heterochromatin regions within chromosome territories remains elusive, because of the complex architecture of the human nucleus. A 3-D analysis of the major histocompatibility complex locus on chromosome 6 revealed megabase-sized loops containing active genes extruding from the chromosome 6 territory (41). Because of structural differences between both genomes, it is yet unclear whether these loops are equivalent to the loops found in *Arabidopsis* nuclei. Based on the genomic sequence (17, 42), we estimate the content of the average chromosome territory of *Arabidopsis* at 25 Mbp of DNA with 5,200 genes, which is

strikingly contrasting with the average human chromosome territory, which contains five times more DNA (130 Mbp) but only ≈1,700 genes.

According to the CC–loop model, some euchromatin regions compartmentalize with CCs, which may affect transcriptional activity in these regions. Heterochromatin-mediated gene silencing is known for *Drosophila* (11, 12), involving Su(var) proteins, and for mammals (13), involving Ikaros proteins. It is tempting to speculate that physical association of gene regions with heterochromatic CCs in *Arabidopsis* may lead to transcriptional inactivation of the corresponding genes.

We observed frequent association of CCs in *Arabidopsis* nuclei, a phenomenon that has been observed in many species, including mammals. In fact, CCs may represent nonrandom spatial association of certain centromeres (39). Furthermore, homologous association of human chromosome territories occurs more frequently for gene-dense, small chromosomes (40). By differential chromosome painting with BAC contigs, we demonstrated homologous association of CCs and chromosome territories. Strikingly, the FISH images revealed perfect alignment of homologous subregions up to a few megabases, possibly controlled by heterochromatin. Heterochromatin has been proposed to play a role in long-range interactions as a matchmaker to promote mitotic alignment of homologs or homologous chromosome regions in *Drosophila* (43), where somatic pairing of homologs seems to be a general phenomenon. Somatic pairing of homologs has been implicated in at least one example of allelic DNA interaction, in this case, tobacco (44), of which there are many examples in plants. Whether heterochromatin generally is involved in somatic transinteraction of homologous DNA sequences remains to be investigated. The *Arabidopsis* nucleus may prove a valuable system with which to investigate these and other fundamental questions on chromosome dynamics and epigenetic regulation mechanisms in plants.

We thank R. van Driel and B. van Steensel for critically reading the manuscript, P. Zabel for valuable discussions, and B. M. Turner (University of Birmingham Medical School, Birmingham, U.K.) for providing antibodies against acetylated histones. This project was supported by grants from the Deutsche Forschungsgemeinschaft (FR 1497/1-1 to P.F.) and the Land Sachsen-Anhalt (3035A/0088B and 2333A/0020B to I.S.).

1. Sadoni, N., Langer, S., Fauth, C., Bernardi, G., Cremer, T., Turner, B. M. & Zink, D. (1999) *J. Cell Biol.* **146,** 1211–1226.
2. Lamond, A. I. & Earnshaw, W. C. (1998) *Science* **280,** 547–553.
3. Karpen, G. H. & Alshire, R. C. (1997) *Trends Genet.* **13,** 489–496.
4. Hennig, W. (1997) *Chromosoma* **108,** 1–9.
5. Jenuwein, T. & Allis, C. D. (2001) *Science* **293,** 1074–1080.
6. Bannister, A. J., Zegerman, P., Partridge, J. F., Miska, E. A., Thomas, J. O., Allshire, R. C. & Kouzarides, T. (2001) *Nature* **410,** 120–124.
7. Noma, K. I., Allis, C. D. & Grewal, S. I. S. (2001) *Science* **293,** 1150–1155.
8. Lachner, M., O'Carroll, N., Rea, S., Mechtler, K. & Jenuwein, T. (2001) *Nature* **410,** 116–120.
9. Schotta, G., Ebert, A., Krauss, V., Fischer, A., Hoffmann, J., Rea, S., Jenuwein, T., Dorn, R. & Reuter, G. (2002) *EMBO J.* **21,** 1121–1131.
10. Jackson, J. P., Lindroth, A. M., Cao, X. F. & Jacobsen, S. E. (2002) *Nature* **416,** 556–560.
11. Csink, A. K. & Henikoff, S. (1996) *Nature* **381,** 529–531.
12. Dernburg, A. F., Broman, K. W., Fung, J. C., Marshall, W. F., Philips, J., Agard, D. A. & Sedat, J. W. (1996) *Cell* **85,** 745–759.
13. Brown, K. E., Amoils, S., Horn, J. M., Buckle, V. J., Higgs, D. R., Merkenschlager, M. & Fisher, A. G. (2001) *Nat. Cell Biol.* **3,** 602–606.
14. Francastel, C., Walters, M. C., Groudine, M. & Martin, D. I. (1999) *Cell* **99,** 259–269.
15. Verschure, P. J., van Der Kraan, I., Manders, E. M. & van Driel, R. (1999) *J. Cell Biol.* **147,** 13–24.
16. Fransz, P., Armstrong, S., Alonso-Blanco, C., Fischer, T. C., Torres-Ruiz, R. A. & Jones, G. (1998) *Plant J.* **13,** 867–876.
17. The Arabidopsis Initiative (2000) *Nature* **408,** 796–815.
18. Martinez-Zapater, J. M., Estelle, M. A. & Somerville, C. R. (1986) *Mol. Gen. Genet.* **204,** 417–423.
19. Heslop-Harrison, J. S., Murata, M., Ogura, Y., Schwarzacher, T. & Motoyoshi, F. (1999) *Plant Cell* **11,** 31–42.
20. Fransz, P. F., Armstrong, S., de Jong, J. H., Parnell, L. D., van Drunen, C., Dean, C., Zabel, P., Bisseling, T. & Jones, G. H. (2000) *Cell* **100,** 367–376.
21. Laibach, F. (1907) *Beih. zum Bot. Centralblatt* **22,** 191–210.
22. Van Blokland, R., Van der Geest, N., Mol, J. M. N. & Kooter, J. M. (1994) *Plant J.* **6,** 861–877.
23. Campell, B. R., Song, Y., Posch, T. E., Cullis, C. A. & Town, C. D. (1996) *Gene* **112,** 225–228.
24. Creusot, F., Fouilloux, E., Dron, M., Lafleuriel, J., Picard, G., Billault, A., Le Paslier, D., Cohen, D., Chaboue, M. E., Durr, A., *et al.* (1996) *Plant J.* **8,** 763–770.
25. Mozo, T., Fischer, S., Meier-Ewert, S., Lehrach, H. & Altmann, T. (1998) *Plant J.* **16,** 377–384.
26. Choi, S., Creelman, R. A., Mullet, J. E. & Wing, R. (1995) *Plant Mol. Biol. Rep.* **13,** 124–128.
27. Richards, E. J. & Ausubel, F. M. (1988) *Cell* **53,** 127–136.
28. Lysak, M. A., Fransz, P. F., Ali, H. B. & Schubert, I. (2001) *Plant J.* **28,** 689–697.
29. Podestá, A., Ruffini Castiglione, M., Avanzi, S. & Montagnoli, G. (1993) *Int. J. Biochem.* **25,** 929–933.
30. Turner, B. M., O'Neill, L. P. & Allan, I. M. (1989) *FEBS Lett.* **253,** 141–145.
31. Jasencakova, Z., Meister, A., Walter, J., Turner, B. M. & Schubert, I. (2000) *Plant Cell* **13,** 2087–2100.
32. Maluszynska, J. & Heslop-Harrison, J. S. (1991) *Plant J.* **1,** 159–166.
33. Dong, F. & Jiang, J. (1998) *Chromosome Res.* **6,** 551–558.
34. Gonzalez-Melendi, P., Beven, A., Boudonck, K., Abranches, R., Wells, B., Dolan, L. & Shaw, P. (2000) *J. Microsc. (Oxford)* **198,** 199–207.
35. Belmont, S. & Bruce, K. (1994) *J. Mol. Biol.* **127,** 287–302.
36. Sachs, R. K., van den Engh, G., Trask, B., Yokota, H. & Hearst, J. E. (1995) *Proc. Natl. Acad. Sci. USA* **92,** 2710–2714.
37. Cook, P. R. (1995) *J. Cell Sci.* **108,** 2927–2935.
38. Munkel, C., Eils, R., Dietzel, S., Zink, D., Mehring, C., Wedemann, G., Cremer, T. & Langowski, J. (1999) *J. Mol. Biol.* **285,** 1053–1065.
39. Manuelides, L. (1985) *Hum. Genet.* **71,** 288–293.
40. Cremer, T. & Cremer, C. (2001) *Nat. Rev. Genet.* **2,** 292–301.
41. Volpi, E. V., Chevret, E., Jones, T., Vatcheva, R., Williamson, J., Beck, S., Campbell, R. D., Goldsworthy, M., Powis, S. H., Ragoussis, J., *et al.* (2000) *J. Cell. Sci.* **113,** 1565–1576.
42. International Human Genome Sequencing Consortium (2001) *Nature* **409,** 860–921.
43. Renauld, H. & Gasser, S. M. (1997) *Trends Cell Biol.* **7,** 201–205.
44. Matzke, M., Mette, M. F., Jakowitsch, J., Kanno, T., Moscone, E. A., van der Winden, J. & Matzke, A. J. (2001) *Genetics* **158,** 451–461.